



Thermodynamic and environmental analyses for paddy drying in a semi-industrial dryer

Mohsen Beigi¹ · Mehdi Torki² · Farhad Khoshnam³ · Mojtaba Tohid⁴

Received: 25 January 2020 / Accepted: 16 June 2020 / Published online: 29 June 2020
© Akadémiai Kiadó, Budapest, Hungary 2020

Abstract

In the present work, the first and second laws of thermodynamics were used to perform energy and exergy analyses for deep bed drying of paddy in a convective dryer. Also, the equivalent specific CO₂ emission was assessed. Drying experiments were carried out at drying air temperatures of 40, 50 and 60 °C, and air flow rates of 0.008, 0.012 and 0.017 m³ s⁻¹. Energy utilization, energy utilization ratio and energy efficiency were obtained to be in the range of 0.061–0.1412 kJ s⁻¹, 22.41–46.81% and 4.37–8.56%, respectively. Exergy loss decreased continually with drying time and the average values ranged from 0.019 to 0.081 kJ s⁻¹. Exergy efficiency varied in the range of 32.44–66.91%. Energy and exergy efficiency was improved at low temperature–low flow rate and high temperature–high flow rate, respectively. The results of environmental analysis declared that specific CO₂ emission ranged from 3.83 to 8.42 kg CO₂ kg_{water}⁻¹ where high temperature–low flow rate drying air reduced the footprint.

Keywords Semi-industrial drying · Rough rice · Energy utilization · Exergy efficiency · CO₂ emission

Introduction

Drying has been known as an effective method to preserve agricultural and food products where the main objective is to prevent microbial spoilage and enhance the shelf life [1]. Generally, it is practically difficult to safe and long storage of fresh agricultural products since the high-water content accelerates enzymatic and metabolic activities and also microorganisms and bacteria growth in the products. By removal large water content from the products, drying process is one of the effective methods to preserve quality of the materials during postharvest period [2]. In addition, to minimizing quality destruction and ensuring safe processing

during further postharvest practices, some agricultural products such as cereal grains must be dried [3].

Thermal drying is the most common method practiced in different industries. Among different thermal methods, convective hot air dryers using fossil fuels are widely used in industrial food applications. The key concern in these systems is high energy consumption [4]. High energy utilization threatens the public health and causes some environmental concerns such as greater emissions of pollutants and warmer global, eutrophication, acid rain, etc. [5]. Therefore, it is necessary to ensure for high energy efficiency as well as desired quality of the final products. In this regard, energy analysis is a useful approach to evaluate required energy as well as energy efficiency in drying systems. The obtained results from the analyzing could be used for determining operative drying parameters, optimizing of the exciting dryers, designing of new dryers, and development of energy recovery systems [6–8].

In thermodynamics, the exergy of a system is defined as the maximum useful work possible during a process that brings the system into equilibrium with a reference environment [9]. Unlike energy, during a process involves a temperature change, exergy is always destroyed. Exergy analysis of thermal systems has been introduced as an effective tool to understand the effect of thermodynamic phenomena on

✉ Mohsen Beigi
mohsenbeigi59@gmail.com

¹ Department of Mechanical Engineering, Tiran Branch, Islamic Azad University, Tiran, Iran

² Department of Electrical and Computer Engineering, Chaharmahal va Bakhtyari Branch, Technical and Vocational University (TVU), Shahrekord, Iran

³ Mechanical Engineering of Biosystems, Faculty of Agricultural, University of Jirof, Jiroft 78671-61167, Iran

⁴ Young Researchers and Elite Club, Shahrekord Branch, Islamic Azad University, Shahrekord, Iran

efficiency, and also to investigate and improve the performance of the systems [10]. In this analysis, the conservation of mass and energy principles together with the second law of thermodynamics is used. In the past decades, some researchers conducted energy and exergy analyses for drying process of different products using various drying systems such as Darvishi et al. [5] for microwave drying of kiwi slices, Prommas et al. [11] for hot air drying of porous media, Akpinar et al. [12] for convective drying of pumpkin, Akbulut and Durmus [13] for forced solar drying of mulberry, and Ranjbaran and Zare [14] for microwave-assisted fluidized bed drying of soybeans, Midilli and Kucuk [15] for solar drying of pistachio, and Aghbashlo et al. [16] for spray drying of fish oil microencapsulation, and Corzo et al. [17] for hot air drying of coroba slices.

Although some new energy and quality efficient methods have been reported for paddy [18–20], but convective fixed deep bed drying is still the most common method used in paddy industry [3]. According to the literature review and to the best of our knowledge, no information was found on combined energy and exergy as well as environmental footprint for deep bed drying of paddy. Therefore, the main objective of the present study was to dry paddy as deep bed at different drying air temperatures and

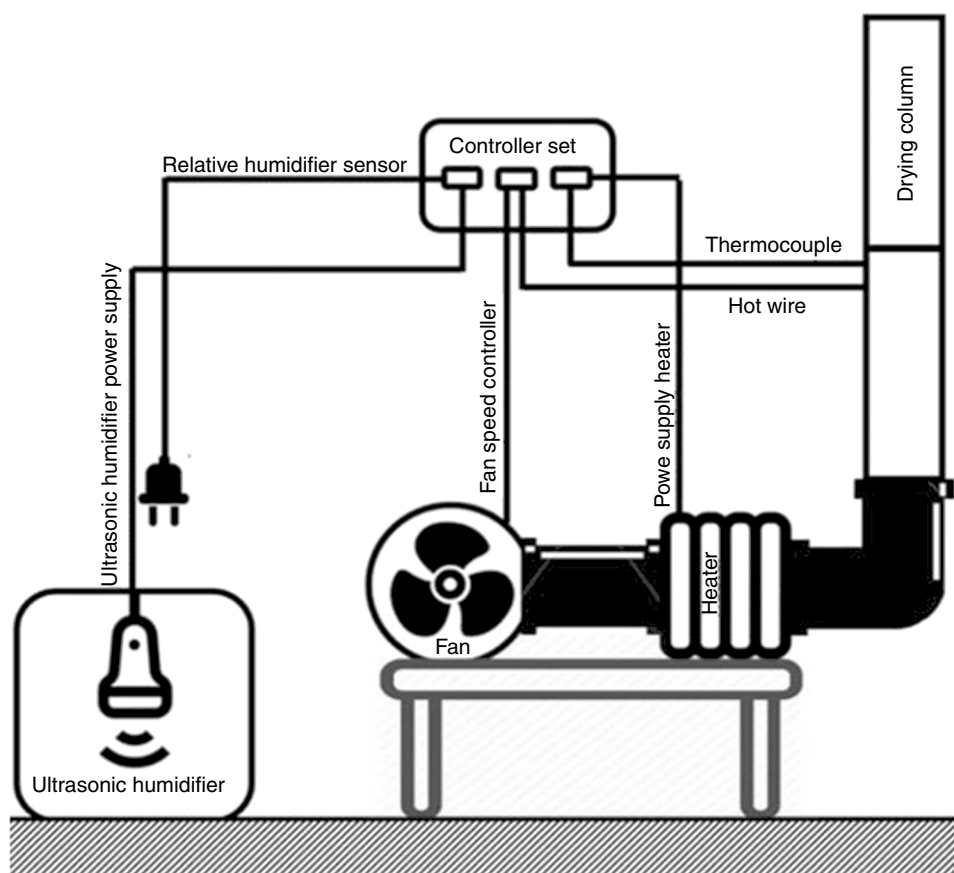
flow rates, and perform thermodynamic and CO₂ emission analyses for the process.

Materials and methods

Experimental

A convective hot air dryer (Fig. 1) was used to perform drying experiments. Specifications of the system components have been specified previously [3]. Drying conditions were selected for different combinations of drying air parameters including temperature (40, 50 and 60 °C) and flow rate (0.008, 0.012 and 0.017 m³ s⁻¹). During the experiments, relative humidity for drying air was remained constant at level of 40%. Deep bed of fresh harvested paddy (with a uniform height of 20 cm) was placed in the drying chamber and variations in the moisture content were monitored by continuous weighing of the samples using a digital laboratory balance with accuracy of 0.01 g (Sartorius 18100P, Sartorius Co., Germany). The drying curves were obtained by computing the instantaneous moisture content using Eq. (1):

Fig. 1 A schematic view of the experimental test rig and instruments



$$M_i = \left(\frac{W_0(M_0 - 1) + W}{W} \right) \tag{1}$$

where M_i and M_0 are the instantaneous and initial moisture contents of drying samples ($\text{kg}_{\text{water}} \text{kg}^{-1}_{\text{wet matter}}$), respectively. Also, W and W_0 are the instantaneous and initial mass (kg) of drying samples, respectively.

In each drying experiment, the samples were dried from an average initial moisture content of $0.20 \text{ kg}_{\text{water}} \text{kg}^{-1}_{\text{wet matter}}$ to a final value of about $0.12 \text{ kg}_{\text{water}} \text{kg}^{-1}_{\text{wet matter}}$.

It is worth to note that, total energy consumption during the process (the consumed energy of heating elements and centrifugal fan) was determined using a digital power meter accurate to 1 J (Zigler Delta Power).

Thermodynamic analyses

By applying the first law of thermodynamics, the rate of energy consumption or energy utilization (EU, kJ s^{-1}) was determined using the following equation [8]:

$$EU = \dot{m}_a(h_{a,i} - h_{a,o}) \tag{2}$$

The mass flow rate of the drying air (\dot{m}_a , kg s^{-1}) was calculated using Eq. (3):

$$\dot{m}_a = A \cdot V_a \cdot \rho_a \tag{3}$$

The density of dry air (ρ_a) was determined as [21]:

$$\rho_a = \frac{101.325}{0.287(T_a + 273.16)} \tag{4}$$

In Eq. (4), A is cross section of the drying chamber (m^2).

The enthalpy (kJ kg^{-1}) of air at inlet and outlet of drying chamber was calculated using Eqs. (5) and (6), respectively [13]:

$$h_{a,i} = C_{pa}T_{a,i} + X_{a,i}h_w \tag{5}$$

$$h_{a,o} = C_{pa}T_{a,o} + X_{a,o}h_w \tag{6}$$

The relative humidity (RH) was converted into humidity ratio as follows [22]:

$$RH = \frac{101.3X}{(0.62189P_{vs} + XP_{vs})} \tag{7}$$

As a function of air temperature (T_a , $^{\circ}\text{C}$), the saturated vapor pressure (P_{vs}) was calculated as follows [21]:

$$P_{vs} = 0.1 \exp \left(27.0214 - \frac{6887}{(T_a + 273.16)} - 5.31 \ln \left(\frac{T_a + 273.16}{273.16} \right) \right) \tag{8}$$

The specific heat of air at constant pressure (C_{pa} , $\text{kJ kg}^{-1} \text{ } ^{\circ}\text{C}^{-1}$) was determined as [22]:

$$C_{pa} = 1.0029 + 5.4 \times 10^{-5}T_a \tag{9}$$

The energy utilization ratio (EUR, %) which is defined as the ratio of energy utilization to the provided energy in the dryer chamber was calculated using Eq. (10) [23]:

$$EUR = \frac{(h_{a,i} - h_{a,o})}{(h_{a,i} - h_{a,\infty})} \times 100 \tag{10}$$

The energy efficiency (η_{energy} , %) was evaluated as follows [11]:

$$\eta_{\text{energy}} = \frac{\dot{m}(h_{a,i} - h_{a,o})}{\dot{m}_a h_{a,i}} \times 100 \tag{11}$$

Exergy analysis of the drying process was performed in light of the second law of thermodynamics and the exergy inflow (Ex_i , kJ s^{-1}), exergy outflow (Ex_o , kJ s^{-1}) and exergy losses (Ex_l , kJ s^{-1}) of the process at steady-state points were determined as follows [24]:

$$Ex_i = \dot{m}_a C_{pa} \left[(T_{a,i} - T_{\infty}) - T_{\infty} \ln \frac{T_{a,i}}{T_{\infty}} \right] \tag{12}$$

$$Ex_o = \dot{m}_a C_{pa} \left[(T_{a,o} - T_{\infty}) - T_{\infty} \ln \frac{T_{a,o}}{T_{\infty}} \right] \tag{13}$$

$$Ex_l = Ex_i - Ex_o \tag{14}$$

Furthermore, the exergy efficiency (η_{exergy} , %) was calculated using Eq. (15) [24]:

$$\eta_{\text{exergy}} = \frac{Ex_o}{Ex_i} \times 100 \tag{15}$$

Equivalent specific CO₂ emission (ESCE)

Khoshnevisan et al. [25] have reported that, in the case of electricity generated by natural gas (LNG), the emission of average CO₂ is about equivalent to 0.61 kg CO_2 per each kWh. Furthermore, the transmission and distribution loss (L_{td}) is taken as 10% and domestic loss (L_d) is considered as 7% for I.R. Iran condition so, the number (X) is changed as follows:

$$X = 0.61 \times \frac{1}{1 - L_{td}} \times \frac{1}{1 - L_d} = 0.73 \tag{16}$$

Therefore, energy consumed for rough rice drying in the practiced convective dryer was converted to its carbon

emission equivalent, and the ESCE ($\text{kg CO}_2 \text{ kg}^{-1} \text{ water}$) was calculated using the following equation:

$$\text{Specific CO}_2 \text{ emission} = \frac{E_t \times 0.73}{m_w} \tag{17}$$

In Eq. (17), E_t is total electrical energy consumption for drying of the samples (kWh). Also, m_w is mass of the evaporated water from drying samples (kg) which was calculated as follows:

$$m_w = \frac{W_0(M_0 - M_f)}{100 - M_f} \tag{18}$$

where M_f is the final moisture contents of drying samples ($\text{kg water kg}^{-1} \text{ wet matter}$).

Uncertainty analysis

Some factors, such as instrument selection, operating condition, data recording, and calibration procedure, could lead to appear uncertainties and errors in experimental studies. Therefore, to demonstrate the repeatability and accuracy of the computed parameters, uncertainty must be analyzed and evaluated. In the present work, the analysis was performed through the use of the Holman methodology using the following equation [26]:

$$W_F = \left[\left(\frac{\partial F}{\partial y_1} w_1 \right)^2 + \left(\frac{\partial F}{\partial y_2} w_2 \right)^2 + \dots + \left(\frac{\partial F}{\partial y_n} w_n \right)^2 \right]^{0.5} \tag{19}$$

Statistical analysis

All the experiments were replicated three times and obtained results subjected to analysis of variance (ANOVA) using SPSS (19.0). The means were compared by practicing Duncan’s multiple range tests ($P < 0.05$).

Results and discussion

Uncertainty analysis

The uncertainties of the experimental measurements as well as the total uncertainties of the investigated thermodynamic and environmental parameters caused by the measurement errors are tabulated in Table 1. As the results show, all the uncertainties pertaining to the thermodynamic and environmental analyses are less the adequate error limit of 5%.

Table 1 Uncertainties of the experimental measurements and overall uncertainties for calculated parameters

| Measurement/parameter | Unit | Uncertainty/% |
|----------------------------------|-----------------------------|---------------|
| <i>Experimental measurements</i> | | |
| Drying air temperature | °C | ±0.668 |
| Drying air flow rate | $\text{m}^3 \text{ s}^{-1}$ | ±0.105 |
| Drying air relative humidity | % | ±0.084 |
| Product mass | g | ±0.01 |
| Process time | s | ±0.025 |
| <i>Calculated parameters</i> | | |
| Energy utilization | kJ s^{-1} | ±3.148 |
| Energy utilization ratio | % | ±2.739 |
| Energy efficiency | % | ±3.857 |
| Inlet exergy rate | kJ s^{-1} | ±1.974 |
| Outlet exergy rate | kJ s^{-1} | ±2.136 |
| Exergy loss rate | kJ s^{-1} | ±2.759 |
| Exergy efficiency | % | ±3.066 |
| CO ₂ emission | kg | ±4.228 |

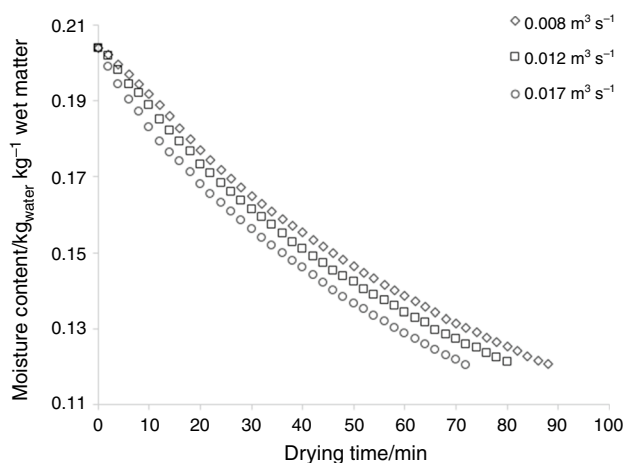


Fig. 2 Variation in moisture content of paddy at constant air temperature of 60 °C and the different practiced air flow rates

Drying kinetics

The typical moisture removal curves for the paddy at different drying air temperatures and flow rates are illustrated in Figs. 2 and 3. The influence of the air flow rate on the process duration can be discussed based on Fig. 2. From the figure, drying duration of the samples was increased with increasing inlet air flow rate. In general, throughout dehydration process of a material in convective hot air drying system, heat and mass transfer phenomena are simultaneously occurred. The air transports energy to the material and takes the evaporated moisture away from the material surface. Nearby the material surface, a district

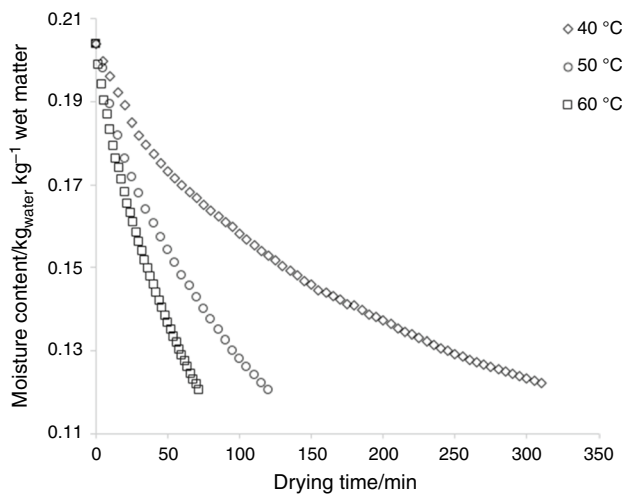


Fig. 3 Variation in moisture content of paddy at constant air flow rate of $0.017 \text{ m}^3 \text{ s}^{-1}$ and the different practiced air temperatures

called boundary layer, pattern of the air stream initially is laminar and then becomes turbulent. The energy transfer in the laminar and turbulent regions is equal to the square root of air velocity and proportional to the velocity (0.8 power), respectively. Throughout drying process, moisture removal from the material is mainly restricted by material itself and the boundary layer. In fact, the boundary layer can be considered as an insulating layer of air limiting the moisture transfer from the product to air. Higher levels of air flow rates decrease the layer resistance leading to faster drying. The same observation in term of the influence of drying air flow rate on drying rate and the process duration has been reported by Zare et al. [18] for paddy in a combined hot air/infrared dryer, Aral and Beşe [27] for convective drying of hawthorn fruit, and Martynenko and Zheng [28] for electrohydrodynamic drying of apple slices.

From Fig. 3 and statistical analysis, dehydration process time was significantly ($P < 0.01$) decreased with increasing drying air temperature where, at constant air flow rate of $0.017 \text{ m}^3 \text{ s}^{-1}$, the duration to reduction in the paddy moisture content from 0.20 to $0.12 \text{ kg}_{\text{water}} \text{ kg}_{\text{wet matter}}^{-1}$ was obtained to be 329, 123 and 79 min, respectively. At higher temperatures, heat transfer between thermal source and the material is accelerated resulting in faster moisture evaporation. Additionally, due to higher interfacial moisture concentration for drying product, driving force for mass transfer enhances with the increasing temperature. The observation is in well agreement with the findings reported by researchers for drying of different biological products such as oyster mushroom in a cabinet-type convective dryer [29], tomato slices in an infrared system [30], and mint leaves in convective dryer [31].

Table 2 Average values of energy utilization (EU) and energy utilization ratio (EUR) for drying process of the paddy

| $T_a/^\circ\text{C}$ | $V_a/\text{m}^3 \text{ s}^{-1}$ | EU/ kJ s^{-1} | EUR/% |
|----------------------|---------------------------------|------------------------|-------|
| 40 | 0.008 | 0.061 | 46.81 |
| | 0.012 | 0.085 | 40.53 |
| | 0.017 | 0.098 | 34.21 |
| 50 | 0.008 | 0.082 | 38.56 |
| | 0.012 | 0.106 | 31.28 |
| | 0.017 | 0.120 | 25.84 |
| 60 | 0.008 | 0.099 | 34.40 |
| | 0.012 | 0.123 | 26.22 |
| | 0.017 | 0.142 | 22.41 |

Energy analysis

The obtained data from the experiments was used to perform energy analysis based on the First law of thermodynamic. Table 2 represents the average values calculated for energy utilization (EU) and energy utilization ratio (EUR). From the results, it can be seen that the energy utilization ranged from 0.061 to 0.142 kJ s^{-1} which is comparable with the results reported in the open literature for drying process of different biological products. Nikbakht et al. [32] performed thermodynamic analyses for microwave-assisted thin layer drying of pomegranate arils and found energy utilization to be in the range of $0.01\text{--}0.27 \text{ kJ s}^{-1}$. Aviara et al. [8] studied native cassava starch drying in a tray dryer and reported energy utilization to be varied from 0.001 to 0.006 kJ s^{-1} .

As shown, energy utilization increased with any increment in both drying air temperature and flow rate where the maximum average energy utilization was obtained at air temperature of $60 \text{ }^\circ\text{C}$ and flow rate of $0.017 \text{ m}^3 \text{ s}^{-1}$, and the minimum value belonged to the temperature of $40 \text{ }^\circ\text{C}$ and flow rate of $0.008 \text{ m}^3 \text{ s}^{-1}$. Higher temperature and flow rate of inlet air increases the inlet enthalpy leads to higher transfer of heat and mass between the air stream and drying product and subsequently, results in more energy utilization. Several researchers have reported similar observation in term of effect of the air temperature and flow rate on energy utilization for convective drying process of different products such as eggplant [23], carrot [4], coroba [17], pomegranate arils [33], and native cassava starch [8].

From Table 2, the energy utilization ratio for deep bed drying of paddy at the practiced drying air conditions changed in the range of 22.41–46.81% which in comparable with the values reported by Nazghelichi et al. [4] for fluidized bed drying of carrot cubes (7.4–48.6%) and Akpinar [34] for parsley leaves in a solar dryer (8.75–41.65%). Furthermore, it is revealed that EUR was reduced with both increasing air temperature and flow rate. The observation is in agreement with the results reported by Aviara et al. [8],

Motevali and Minaei [33], Erbay and Icier [35], and Akpinar et al. [12]. It is worth to note that, unlike the findings, some researchers have reported different observation. For example, Corzo et al. [17] noted that the energy utilization ratio for drying of coroba slices in a convective type dryer enhanced with increasing drying temperature up to a point and then reduced with further increment in the temperature.

Figure 4 represents variations of energy utilization and energy utilization ratio as a function of drying time for drying air temperature of 60 °C and different flow rates. From the figure, instantaneous EU and EUR values decreased continually with drying time. For the other drying conditions practiced in the present work, the same trends were observed. At beginning and also early minutes of the process, due to meaningful gradients, the heat and mass transfer between the hot air and the moist product are significant. Therefore, difference between input and output enthalpies is high leading to great energy utilization (according to Eqs. 2, 5 and 6). As the process continues, the air and product approach the temperature equilibrium as well as the product moisture content is decreased. The phenomena result in reduced difference between the input and output enthalpies

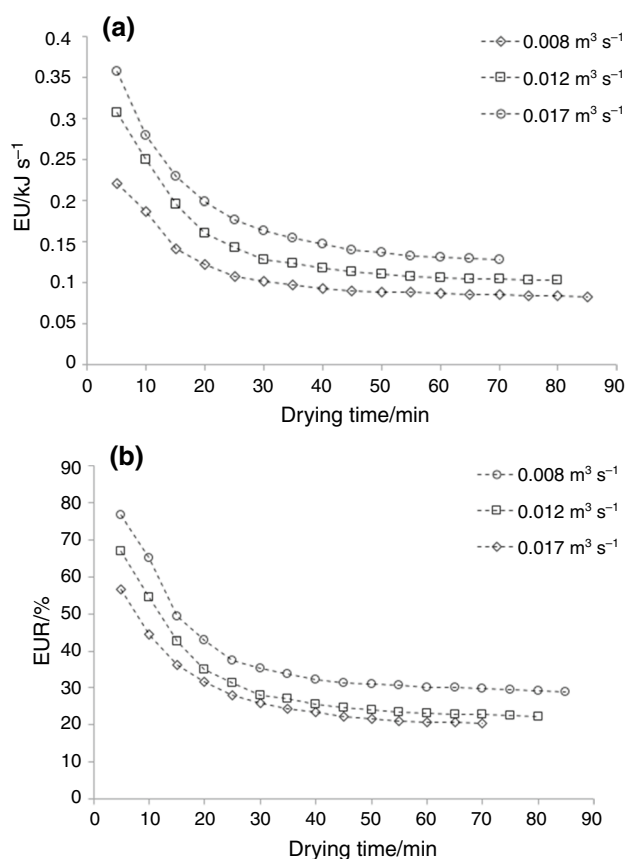


Fig. 4 Variations of energy utilization (EU) (a) and energy utilization ratio (EUR) (b) during the paddy drying at constant air temperature of 60 °C and different air flow rates

and consequently energy utilization is decreased. To delay and or advance the threshold point, temperature and flow rate of drying air could be changed. The same findings have been reported in the literature by several researchers for drying of different agricultural and food products [12, 26, 27].

Average values determined for the energy efficiency of paddy drying are presented in Fig. 5. From the obtained results, the average energy efficiency values varied from 4.37 to 8.56%. The energy efficiencies are comparable with the results reported by Darvishi et al. [5] for microwave drying of kiwi slices (15.15–32.27%), Aviara et al. [8] for solar tray drying of cassava starch (16.04–32.65%), Aghbashlo et al. [16] for spray drying of fish oil microencapsulation (7.49–8.53%), and Surendhar et al. [36] for microwave drying of turmeric slices.

From Fig. 5, any increment in both drying air temperature and flow rate decreased the energy efficiency. At a constant temperature of inlet air, higher flow rate causes shorter heat transfer time between the air and product leading to warmer outlet air. The phenomenon results in higher enthalpy of the air at outlet of drying chamber and consequently, decreases the energy efficiency. In other words, higher inlet air flow rates vent the major portion of inlet energy to the environment without useful application and therefore, decrease the energy efficiency [26]. Furthermore, according to Eq. (11), the observation is reasonable because of inverse relation between the energy efficiency and inlet energy to drying chamber [16].

Exergy analysis

Exergy loss for the paddy drying was calculated by using Eq. (14), and the determined average values are presented in Fig. 6. As shown, exergy loss decreased with both increasing

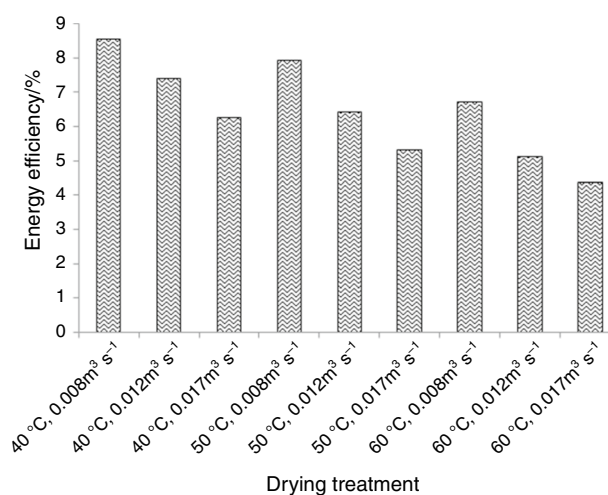


Fig. 5 Effect of drying air temperature and flow rate on energy efficiency for the paddy drying

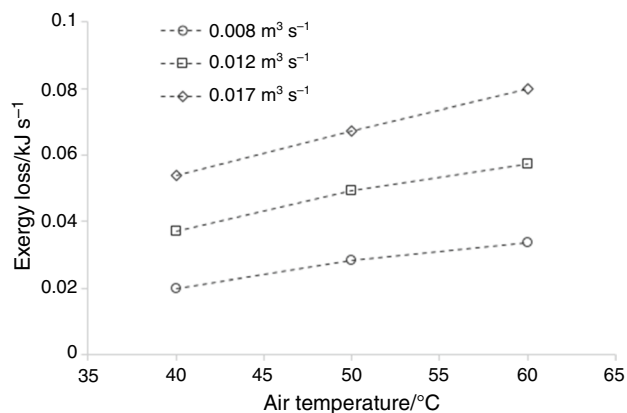


Fig. 6 Effect of drying air temperature and flow rate on exergy loss for the paddy drying

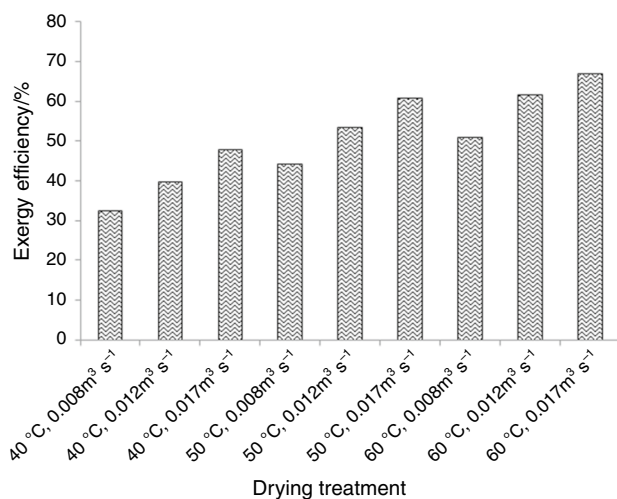


Fig. 7 Effect of drying air temperature and flow rate on exergy efficiency for the paddy drying

drying air temperature and flow rate where the minimum (0.019 kJ s^{-1}) and maximum (0.081 kJ s^{-1}) values of exergy loss were obtained at air temperature of $40 \text{ }^{\circ}\text{C}$ and flow rate of $0.008 \text{ m}^3 \text{ s}^{-1}$, and temperature of $60 \text{ }^{\circ}\text{C}$ and air flow rate of $0.017 \text{ m}^3 \text{ s}^{-1}$. Higher drying air temperature and flow rate caused more exergy loss due to the larger quantity of entering exergy into drying chamber and more part of inflow exergy utilized to evaporate water from the product [4]. Similar results have been reported in the open literature by some researchers, e.g., Motevali and Minaei [33] for thin layer drying of sour pomegranate arils, Erbay and Icier [35] for drying of olive leaves in a tray dryer, Corzo et al. [17] for thin layer drying of coroba slice and Akpınar [37] for convective drying of red pepper slices.

Exergy efficiency for the process was calculated by using Eq. (15) and the average values are represented in Fig. 7.

The average exergy efficiency varied from 32.44% (for air temperature of $40 \text{ }^{\circ}\text{C}$ and $0.008 \text{ m}^3 \text{ s}^{-1}$) to 66.91% (for air temperature of $60 \text{ }^{\circ}\text{C}$ and $0.017 \text{ m}^3 \text{ s}^{-1}$). The obtained values are comparable with the exergy efficiencies reported in the literature for drying of red pepper slices (85.64–88.32%) [37], fish oil microencapsulation (5.26–7.42%) [16], kiwi slices (11.35–24.68%) [5], and red seaweed (30%) [38].

The influences of inlet air temperature and flow rate on the exergy efficiency of paddy drying are further represented in Fig. 7. As shown, the exergy efficiency increased following the augment in both the drying air temperature and flow rate. At higher air flow rates, inlet air passes the drying chamber faster and is not enough time for effective heat transfer between the air and the product. Therefore, temperature of the outlet air is increased leading to higher outlet exergy (Eq. 13) and higher exergy efficiency. Furthermore, in case of the influence of drying air temperature on the exergy efficiency, the observation is reasonable due to the fact that the increase in the drying air temperature enhances the quantity of exergy inlet to the drying chamber, and subsequently the main portion of the inlet exergy is vented by the outlet air without any use for water evaporation. In other words, higher inlet air temperature ensued more increase in the exergy outlet comparisons with the exergy rate of the inlet air. Similar observation has been reported by Akpınar et al. [12], Corzo et al. [17], Nazghelichi et al. [4] and Aviara et al. [8].

It is worth to note that, in addition to temperature and flow arte, relative humidity of drying air could affect the exergy efficiency. In some cases, the energy content of hot moist air may not be directly usable due to its high humidity. Most conventional dryers in agricultural processing waste a lot of heat through the exhaust air. Therefore, as the exergy efficiency is only dependent on the air temperature at inlet and outlet of drying chamber (Eqs. 12, 13 and 15), it could be concluded that the exergy efficiency enhances with the increasing air humidity.

Furthermore, the exergy efficiency curves for some randomly selected conditions are presented in Fig. 8. As shown, the exergy efficiency increased continually with the drying time. The influence of drying air temperature and flow rate on exergy efficiency of the drying process can also be seen from the figure. The same trend was observed for other drying conditions.

Emission of carbon dioxide

The average specific CO_2 emission for deep bed dehydration of paddy at the practiced inlet air conditions are represented in Fig. 9. As shown, the equivalent CO_2 emission to remove 1 kg water of the samples was calculated to be changed from 3.83 to $8.42 \text{ kg CO}_2 \text{ kg}_{\text{water}}^{-1}$. From the results, increasing drying air velocity led to significant ($P < 0.05$) increment in

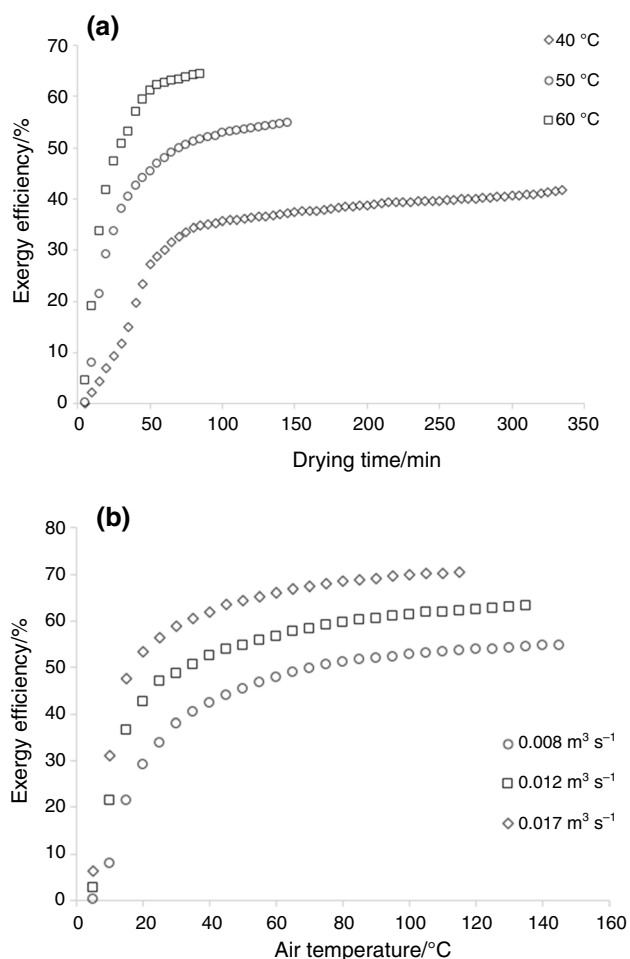


Fig. 8 Variations of exergy efficiency during the paddy drying at constant air flow rate of $0.008 \text{ m}^3 \text{ s}^{-1}$ (a), and constant temperature of $50 \text{ }^\circ\text{C}$ (b)

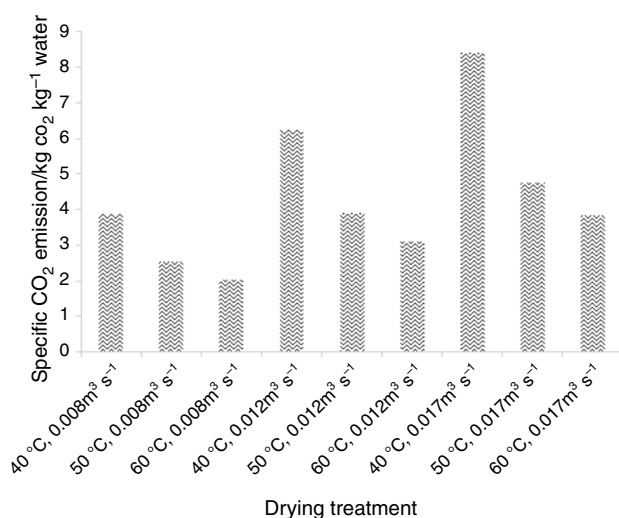


Fig. 9 Effect of drying air temperature and flow rate on average specific CO_2 emission for the paddy drying

CO_2 emission. As mentioned before, due to lack of enough time for effective heat transfer between the air and the product, the most portion of the inlet energy exhausts the drying chamber. Therefore, although the process time is decreased with increasing inlet drying air flow rate, however, energy required to dry the material is generally enhanced. Furthermore, the obtained results showed that the specific CO_2 emission was significantly ($P < 0.05$) decreased at higher drying air temperatures.

Although the increasing air temperature results in a decrement and an increment in the process time and specific heat of air, respectively, but the influence of shortened dehydration duration at higher temperatures is more important than the effect of increased specific heat capacity. Therefore, lower energy is consumed at higher drying air temperatures [39].

Conclusions

In this study, the influence of drying air temperature and flow rate on thermodynamic and environmental indices of paddy drying was investigated. Considering the obtained results and findings, the following conclusions can be drawn from the work:

- Using low temperature—low flow rate scheme for drying air resulted in higher energy efficiency.
- Average exergy loss enhanced with the both increasing air temperature and flow rate.
- Exergy efficiency ranged from 32.44 to 66.91% where, due to greater values of exergy outflow from the drying chamber, higher temperatures and higher flow rate of inlet air improved the efficiency.
- The specific CO_2 emission during the drying experiments rose from 3.83 to $8.42 \text{ kg CO}_2 \text{ kg}_{\text{water}}^{-1}$ owing to the increment in the flow rate and decrement in the temperature of the inlet drying air.

Acknowledgements The authors are deeply grateful to the Language Center of Tiran Branch, Islamic Azad University, to finalize the manuscript.

References

1. Süfer Ö, Palazoğlu TK. A study on hot-air drying of pomegranate: kinetic of dehydration, rehydration and effects on bioactive compounds. *J Therm Anal Calorim.* 2019;137:1981–90.
2. Selimefendgil F, Çoban SÖ, Öztöp HF. Convective drying of a moist porous object under the effects of a rotating cylinder in a channel. *J Therm Anal Calorim.* 2019. <https://doi.org/10.1007/s10973-019-09140-5>.

3. Tohidi M, Sadeghi M, Torki-Harchegani M. Energy and quality attributes for fixed deep bed drying of paddy. *Renew Sustain Energy Rev.* 2017;70:519–28.
4. Nazghelichi T, Kianmehr MH, Aghbashlo M. Thermodynamic analysis of fluidized bed drying of carrot cubes. *Energy.* 2010;35:4679–84.
5. Darvishi H, Zarein M, Farhudi Z. Energetic and exergetic performance analysis and modeling of drying kinetics of kiwi slices. *J Food Sci Technol.* 2016;53:2317–33.
6. Aghbashlo M, Mobli H, Rafiee S, Madadlou A. A review on exergy analysis of drying processes and systems. *Renew Sustain Energy Rev.* 2013;22:1–22.
7. Singh RP. Energy consumption and conservation in food sterilization. *Food Technol.* 1977;31:57–60.
8. Aviara NA, Onuoha LN, Falola OE, Igbeka JC. Energy and exergy analyses of native cassava starch drying in a tray dryer. *Energy.* 2014;73:809–17.
9. Syahrul S, Hamdullahpur F, Dincer I. Exergy analysis of fluidized bed drying of moist particles. *Exergy Int J.* 2002;2:87–98.
10. Dincer I. Exergy as a potential tool for sustainable drying systems. *Sustain Cities Soc.* 2011;1:91–6.
11. Prommas R, Rattanadecho P, Cholaseul D. Energy and exergy analyses in drying process of porous media using hot air. *Int Commun Heat Mass Transf.* 2010;37:372–8.
12. Akpınar EK, Midilli A, Bicer Y. The first and second law analyses of thermodynamic of pumpkin drying process. *J Food Eng.* 2006;72:320–31.
13. Akbulut AO, Durmus A. Energy exergy analysis of thin layer drying of mulberry in a forced solar dryer. *Energy.* 2010;35:1754–63.
14. Ranjbaran M, Zare D. Simulation of energetic- and exergetic performance of microwave-assisted fluidized bed drying of soybeans. *Energy.* 2013;59:484–93.
15. Midilli A, Kucuk H. Energy and exergy analyses of solar drying process of pistachio. *Energy.* 2003;28:539–56.
16. Aghbashlo M, Mobli H, Rafiee S, Madalou A. Energy and exergy analyses of the spray drying process of fish oil encapsulation. *Biosyst Eng.* 2012;111:229–41.
17. Corzo O, Bracho N, Vásquez A, Pereira A. Energy and exergy analyses of thin layer drying of coroba slices. *J Food Eng.* 2008;86:151–61.
18. Zare D, Naderi H, Ranjbaran M. Energy and quality attributes of combined hot-air/infrared drying of paddy. *Dry Technol.* 2015;33:570–82.
19. Sangdao C, Songsermpong S, Krairiksh M. A continuous fluidized bed microwave paddy drying system using applicators with perpendicular slots on a concentric cylindrical cavity. *Dry Technol.* 2011;29:35–46.
20. Soponronnarit S, Prachayawarakorn S, Rordprapat W, Nathakarakankule A, Tia W. A superheated-steam fluidized-bed dryer for parboiled rice: testing of a pilot-scale & mathematical model development. *Dry Technol.* 2006;24:1457–67.
21. Naghavi Z, Moheb A, Ziaei-rad S. Numerical simulation of rough rice drying in a deep-bed dryer using non-equilibrium model. *Energy Convers Manag.* 2010;51:258–64.
22. Zare D, Minaei S, Mohamad Zade M, Khoshtaghaza MH. Computer simulation of rough rice drying in a batch dryer. *Energy Convers Manag.* 2006;47:3241–54.
23. Akpınar EK. Energy and exergy analyses of drying of eggplant slices in a cyclone type dryer. *J Mech Sci Technol.* 2005;19:692–703.
24. Kesavan S, Arjunan TV, Vijayan S. Thermodynamic analysis of a triple-pass solar dryer for drying potato slices. *J Therm Anal Calorim.* 2019;136:159–71.
25. Khoshnevisan B, Rafiee S, Iqbal J, Shamshirband Sh, Omid M, Badrul Anuar N, Abdul Wahab AW. A comparative study between artificial neural networks and adaptive neuro-fuzzy inference system for modeling energy consumption in greenhouse tomato production: a case study in Isfahan province. *J Agric Sci Technol.* 2015;17:49–62.
26. Beigi M, Tohidi M, Torki-Harchegani M. Exergetic analysis of deep-bed drying of rough rice in a convective dryer. *Energy.* 2017;140:374–82.
27. Aral S, Bese AV. Convective drying of hawthorn fruit (*Crataegus* spp.): effect of experimental parameters on drying kinetics, color, shrinkage, and rehydration capacity. *Food Chem.* 2016;210:577–84.
28. Martynenko A, Zheng W. Electrohydrodynamic drying of apple slices: energy and quality aspects. *J Food Eng.* 2016;168:215–22.
29. Tulek Y. Drying kinetics of oyster mushroom (*Pleurotus ostreatus*) in a convective hot air dryer. *J Agric Sci Technol.* 2011;13:655–64.
30. Sadin R, Chegini GR, Sadin H. The effect of temperature and slice thickness on drying kinetics tomato in the infrared dryer. *Heat Mass Transf.* 2014;50:501–7.
31. Beigi M. Drying of mint leaves: influence of the Process temperature on dehydration parameters, quality attributes, and energy consumption. *J Agric Sci Technol.* 2019;21:77–88.
32. Nikbakht AM, Motevali A, Minaei S. Energy and exergy investigation of microwave assisted thin-layer drying of pomegranate arils using artificial neural networks and response surface methodology. *J Saudi Soc Agric Sci.* 2014;13:81–91.
33. Motevali A, Minaei S. Effects of microwave pretreatment on the energy and exergy utilization in thin-layer drying of sour pomegranate arils. *Chem Ind Chem Eng Q.* 2012;18:63–72.
34. Akpınar EK. Drying of parsley leaves in a solar dryer and under open sun: modeling, energy and exergy aspects. *J Food Process Eng.* 2011;34:27–48.
35. Erbay Z, Icier F. Energy and exergy analysis on drying of olive leaves (*Olea europaea* L.) in tray drier. *J Food Process Eng.* 2011;34:2105–23.
36. Surendhar A, Sivasubramanian V, Vidhyeswari D, Deepanraj B. Energy and exergy analysis, drying kinetics, modeling and quality parameters of microwave-dried turmeric slices. *J Therm Anal Calorim.* 2019;136:185–97.
37. Akpınar EK. Energy and exergy analyses of drying of red pepper slices in convective type dryer. *Int Commun Heat Mass Transf.* 2004;31:1165–76.
38. Fudholi A, Sopian K, Othamn MY, Ruslan MH. Energy and exergy analyses of solar drying system of red seaweed. *Energy Build.* 2014;68:121–9.
39. Ghanbarian D, Torki-Harchegani M, Sadeghi M, Ghasemi Pirbalouti A. Ultrasonically improved convective drying of peppermint leaves: influence on the process time and energetic indices. *Renew Energy.* 2020;153:67–73.

Publisher's Note Springer Nature remains neutral with regard to jurisdictional claims in published maps and institutional affiliations.